Quantum many-body theories about the crust of neutron stars

Ulysses Zhan*
Department of Physics, University of California, Santa Barbara
(Dated: December 12, 2024)

This paper reviews some the quantum many-body theories relevant to the neutron star crust. The outer crust consists of iron-like nuclei in a lattice structure surrounded by relativistic electrons, modeled as a one-component plasma. The inner crust, located above the neutron drip point, contains free neutrons forming Cooper pairs, leading to superfluidity. Magnetic fields also play a critical role, quantizing electron motion and influencing crustal properties.

I. Introduction

Born in catastrophic gravitational core-collapse supernova explosions, neutron stars are the densest stars known in the universe [1]. Studying the neutron star crust is crucial for modelling magnetar radiation [2], glitches [3], gravitational wave emission [4], and other astrophysical phenomena. Different approaches have been used to model the neutron star crust in different aspects, including using solid mechanics [5], thermodynamics [6], and fluid dynamics [7]. In this article, we will focus on the quantum many-body theories that describe the crust of a neutron star.

The neutron star crust is defined [8] as the region in the neutron star where the density is below the nuclear saturation density $\rho_0 \approx 2.5 \times 10^{17}\,\mathrm{kg\,m^{-3}}$, which is defined as that minimizing the energy density of an infinite nuclear matter [9]. For higher density (which is outside the scope of the present article), the properties of the matter is much less understood [1, p. xxii], but there are works that theorize them as nearly-pure neutron plasma [8] or quark–gluon plasma [10].

Because the density in the crust is below the nuclear saturation density, nuclei can form. In the outer crust, they will primarily be ^{56}Fe because it has the highest binding energy per nucleon [11] (though some claim that it may not consist of iron [12]). The nuclei are more neutron rich as the density increases due to electron captures [13]. The nuclei form a lattice structure, which is explained in Section II.

The crust is further divided into the outer and inner crusts, separated by the neutron drip point $\rho_{\mathrm{ND}} \approx 4.3 \times 10^{14}\,\mathrm{kg\,m^{-3}}$, above which it is energetically favorable for neutrons to leak from nuclei to become free neutrons [14]. The cause and implications are discussed in Section III. Those neutrons can form Cooper pairs and form a superfluid, which is discussed in Section V.

II. Lattice structure

As stated in the introduction, the outer crust consists of nuclei (assuming number density n_{N}). To make the substance electrically neutral, there are also electrons with number density $n_{\mathrm{e}} = Zn_{\mathrm{N}}$ (where Z is the charge number of the nucleus). A simple calculation shows that for density at $\rho \sim 10^8\,\mathrm{kg\,m^{-3}}$, the electron Fermi momentum (assuming ideal gas) is

$$p_{\mathrm{Fe}} = \hbar \left(3\pi^2 n_{\mathrm{e}}\right)^{1/3} \sim 10^{-1} m_{\mathrm{e}} c,$$

which means that the electrons are relativistic beyond this density. One may also assume that atoms are fully ionized at this density due to pressure ionization [15]. Therefore, we can model the matter as a one-component plasma (OCP) of nuclei immersed in an ideal relativistic electron gas.

Theories about OCP can then be applied. Classically, almost all thermodynamic properties, including phase changes, of an OCP is controlled by a single parameter called the plasma coupling parameter Γ [16], defined as the ratio of the Coulomb energy to the thermal energy:

$$\Gamma = \frac{(Ze)^2/a}{k_{\mathrm{B}}T},$$

where the inter-particle spacing a can be taken as the Wigner–Seitz radius $a \coloneqq (3/4\pi n_{\mathrm{N}})^{1/3}$. The melting point value Γ_{m} is 172–178 from Monte Carlo simulations and corrections [17].

Quantum treatment is needed to find a more accurate value of Γ_{m}. The zero-point quantum vibrations of ions lead to larger Γ_{m}. Currently theory on quantum OCP solid is to use the Einstein model for the longitudinal sound mode (single vibrational frequency) and to use the Debye model for the two transverse sound modes (linear dispersion). The frequency of the longitudinal mode and the sound speed of the transverse modes are determined by the classical limit and Kohn's sum rule [18]. The melting condition is then estimated using the Lindemann melting criterion [19]. It turns out that, to describe the condition of crystallization, one needs another parameter in additional to Γ, which can be chosen as $r_{\mathrm{s}} \coloneqq a/a_0$, where $a_0 \coloneqq \hbar/m(Ze)^2$ is the ionic Bohr radius. The full equation is given by [19]. A comparison between this theoretical result and simulations is given by [20]. A phase diagram is shown in FIG. 1.

If we assume that the temperature is zero, which one may expect to be a valid approximation for neutron stars that have been cooling for a long time (not true for young

* youqiu@ucsb.edu

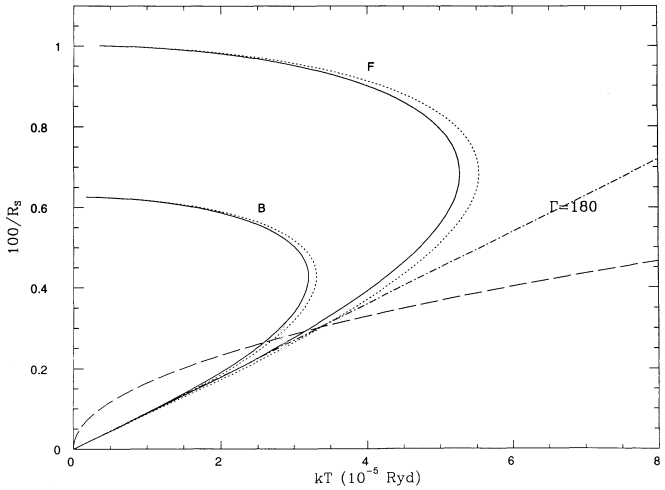

FIG. 1. Phase diagram of the one-component plasma adapted from [19]. The two solid curves corresponds to the fluid–solid coexistence lines of bosons and fermions respectively. The dot-dashed line is the classical melting line. Other lines on the diagram are not important for the present discussion, but one may refer to the original paper for more details.

neutron stars (10^{10} K [21]) and accreting neutron stars), we can infer the type of nuclei and the type of lattice structure by minimizing the energy. The energy consists of the lattice energy (see [22] for calculations), the electron energy (using the model of relativistic Fermi gas), and the nucleus binding energy (see [23] for formulas). Major difficulties in this method do not involve quantum many-body theories, so we will not discuss them in the present article. One may find details of this method in [24].

For more general consideration, the crystal consists of a mixture of nuclei. This is because at finite temperature, the composition is actually a statistical distribution of A and Z [25]. Complex composition can make it have a variety of phases [26]. Even for low temperature, the composition can be "frozen in" after crystallization and thus be different from the actual ground state [24].

III. Free neutrons

As stated in the introduction, the inner crust is beyond the neutron drip point and consists of free neutrons. The reason for the existence of free neutrons is as follows [13]. The electron capture reaction is

$$ {}^{A}_{Z}\mathrm{X} + \Delta Z\, \mathrm{e}^- \longrightarrow {}^{A}_{Z-\Delta Z}\mathrm{Y} + \Delta Z\, \nu_\mathrm{e}. $$

Because the electron gas is degenerate, it becomes energetically favorable for the electrons to be captured by the nuclei (undergoing the above reaction) as the density increases, so the nuclei become more neutron rich. When the nuclei are neutron rich enough (defining the neutron drip point), they are unstable against neutron emission [27]

$$ {}^{A}_{Z-\Delta Z}\mathrm{Y} \longrightarrow {}^{A-\Delta N}_{Z-\Delta Z}\mathrm{Y} + \Delta N\, \mathrm{n} $$

and creates free neutrons in this process.

Therefore, to model the inner crust, one must consider free neutrons. Some instructive models include the liquid drop model [28], semiclassical density functional theory, and density matrix expansion. The liquid drop model is classical, so we will not discuss it in the present article.

The model involving semiclassical density functional theory expresses the energy density as a functional of the number densities of protons, neutrons, and electrons:

$$ \varepsilon = \varepsilon_\mathrm{N}[n_\mathrm{n}, n_\mathrm{p}] + \varepsilon_\mathrm{e}[n_\mathrm{e}] + \varepsilon_\mathrm{Coul}[n_\mathrm{e}, n_\mathrm{p}]\,, $$

where $\varepsilon, n_\mathrm{n}, n_\mathrm{p}, n_\mathrm{e}$ are functions of position, and $\varepsilon_\mathrm{N}, \varepsilon_\mathrm{e}, \varepsilon_\mathrm{Coul}$ are functionals corresponding to nuclear, electron, and Coulomb contributions. The $\varepsilon_\mathrm{Coul}$ part is well-studied: it consists of the classical electrostatic energy and the quantum exchange-correlation energy given by the Slater–Kohn–Sham functional [29]. The ε_e part is easy: it is just the kinetic energy in the Thomas–Fermi model [30, p. 5]. The ε_N part is the most difficult and not well-formulated. The current most popular model is the Hartree–Fock approximation to the generalized Skyrme interaction [24], constructed from adding more terms to the original Skyrme interaction [31], which in turn follows from a low-energy effective field theory of quantum chromodynamics [32]. Though its expression is very complicated, it can be written in a form of local interaction, which makes it easy to work with. For details of the semiclassical model of density functional theory, one may refer to [33].

The density matrix expansion is a quantum many-body theory that uses relative and center-of-mass coordinates to expand the particle number density matrix ρ and the kinetic energy density matrix τ, defined as

$$ \rho(\mathbf{R}_1, \mathbf{R}_2) = \sum_a \varphi_a(\mathbf{R}_1)^*\, \varphi_a(\mathbf{R}_2)\,, $$
$$ \tau(\mathbf{R}_1, \mathbf{R}_2) = \sum_a \nabla\varphi_a(\mathbf{R}_1)^* \cdot \nabla\varphi_a(\mathbf{R}_2)\,, $$

where φ_a are the wave functions labeled by quantum number a representing different single-particle states. To avoid confusion, the so-called density matrix ρ is not related to the density matrix in quantum mechanics. The expansion refers to writing it as [34]

$$ \rho\Big(\mathbf{R} + \frac{\mathbf{s}}{2}, \mathbf{R} - \frac{\mathbf{s}}{2}\Big) = \mathrm{e}^{\mathbf{s}\cdot(\nabla_1 - \nabla_2)/2} \rho(\mathbf{R}_1, \mathbf{R}_2)\Big|_{\mathbf{R}_1 = \mathbf{R}_2 = \mathbf{R}}\,, $$

where $\nabla_{1,2}$ acts on $\mathbf{R}_{1,2}$ respectively. This expansion can be modified to utilize the spherical Bessel functions. Based on this expansion, similar expansion can also be done for higher-order connections like

$$ \rho\Big(\mathbf{R} + \frac{\mathbf{s}}{2}, \mathbf{R} + \frac{\mathbf{t}}{2}\Big)\, \rho\Big(\mathbf{R} - \frac{\mathbf{s}}{2}, \mathbf{R} - \frac{\mathbf{t}}{2}\Big)\,. $$

This enables one to express non-local interactions in the expression of nuclear energy in a local form. With some arguments, one can throw away most terms in the expansion, and derive the following form for the nuclear energy density (in units of $\hbar^2/2m$) [35]:

$$H = \tau_\mathrm{n} + A + B\tau_\mathrm{n} + C\left|\nabla\rho_\mathrm{n}\right|^2 + D\nabla\rho_\mathrm{n}\cdot\nabla\rho_\mathrm{p} + \mathrm{n}\leftrightarrow\mathrm{p},$$

where $\rho_{\mathrm{n,p}}(\mathbf{R}) \coloneqq \rho_{\mathrm{n,p}}(\mathbf{R},\mathbf{R})$ for neutrons and protons respectively and similarly for $\tau_{\mathrm{n,p}}$, and A, B, C, D are local functionals of $\rho_{\mathrm{n,p}}$. For the full Hamiltonian, one also needs to include the the Coulomb energy, spin–orbit coupling, and effective contribution from Pauli exclusion. After the Wigner–Seitz approximation, which assumes that the matter consists of spheres with radius a defined in the previous section [36], the Schrödinger equation takes the form [37]

$$-\nabla\cdot\frac{\hbar^2}{2m_q^{\mathrm{eff}}(r)}\nabla\varphi_a^{(q)}(\mathbf{r}) + U_q(r)\,\varphi_a^{(q)}(\mathbf{r}) + \frac{W_q(r)}{r}\mathbf{l}\cdot\boldsymbol{\sigma}\varphi_a^{(q)}(\mathbf{r}) = \epsilon_a^{(q)}\varphi_a^{(q)}(\mathbf{r}),$$

where $q = \mathrm{n,p}$ denotes neutrons and protons respectively; $\mathbf{l} \coloneqq -\mathrm{i}\mathbf{r}\times\nabla$ is the dimensionless angular momentum operator; and $\boldsymbol{\sigma}$ are the Pauli matrices. The functions $m_q^{\mathrm{eff}}, U_q, W_q$ all depend on ρ_q, τ_q, and the spin–orbit densities

$$\mathbf{J}_q(\mathbf{r}) \coloneqq \mathbf{r}\sum_a \varphi_a^{(q)}(\mathbf{r})^*\,\frac{\mathbf{l}\cdot\boldsymbol{\sigma}}{r^2}\varphi_a^{(q)}(\mathbf{r}).$$

This Schrödinger equation can be solved by reducing it into ordinary differential equations by writing it on the basis of the total angular momentum. One can also solve this equation with Floquet periodicity boundary condition in a unit cell of the nuclei lattice to find a band structure of neutron waves.

For both the semiclassical method and the density matrix expansion method, one can determine the sturcture of the inner crust by minimizing the energy per nucleon. FIG. 2 shows the composition of the inner crust calculated by different authors using semiclassical models, and FIG. 3 shows the composition calculated by different authors using quantum models. Those two figures are adapted from [38]. For more details, one may refer to the citations in the figure captions.

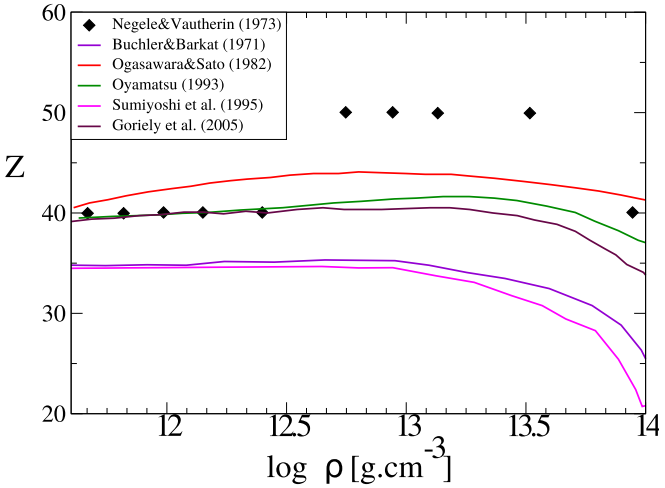

FIG. 2. Proton number of nuclei versus density in the ground state of the inner crust calculated by various authors using semiclassical models: Buchler [39], Ogasawara [40], Oyamatsu [41], Sumiyoshi [42], Goriely [43]. For comparison, the results of quantum calculations from Negele [44] are also included. Figure adapted from [38].

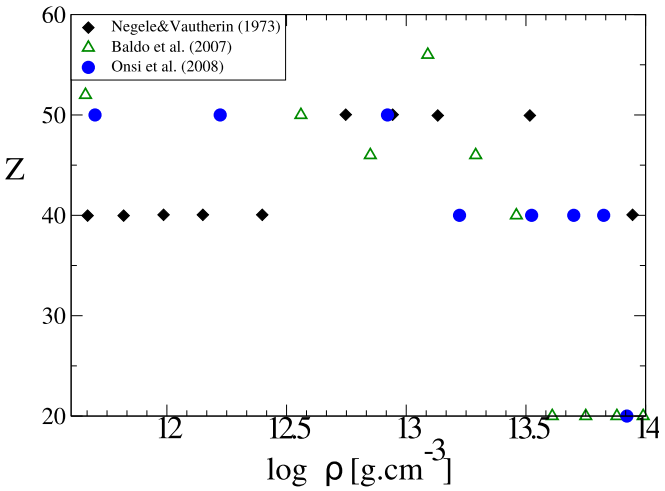

FIG. 3. Proton number of nuclei versus density in the ground state of the inner crust calculated by various authors using quantum models: Negele [44], Baldo [45, 46], Onsi [47]. Figure adapted from [38].

IV. Magnetic field

Typical neutron stars have surface magnetic fields of 10^{11}–10^{15} G [1, pp. xxi, 12], which is stronger than any other magnetic fields that humans or nature creates. The origin of this magnetic field is unclear [48].

The direct impact of the magnetic field is that the electron motion perpendicular to the field is quantized in Landau–Rabi levels [49]

$$E_n = \sqrt{c^2p_z^2 + m_\mathrm{e}^2c^4\,(1+2nB_\star)}, \quad n = 0, 1, \ldots,$$

where $B_\star \coloneqq B/B_\mathrm{c}$ with $B_\mathrm{c} \coloneqq m_\mathrm{e}^2c^2/\hbar e \approx 4.4\times10^{13}$ G.

Magnetic field induced condensed matter can form [50]. Because electron motion is confined to a Landau level, Atoms have a cylindrical shape and can form linear chains along the magnetic field, the attraction between which leads to a condensed phase. There is a critical temperature below which the phase forms at zero pressure. To study this matter, the species of particles in the vapor that one needs to consider include ions (Fe^{n+}), molecules (Fe_n), and electrons (the nucleus Fe is chosen for example; one can replace it with generic ${}^A_Z\mathrm{X}$). Ions and molecules are treated as classical ideal gases, and the electrons are

treated as Fermi gas livinig in the Landau levels. The reason that ions are not confined in Landau levels is that the cyclotron frequency for nucleus is much smaller than that of electrons. With the total density of the vapor fixed, the density of each species in the vapor can be determined by requiring the equilibrium of the reactions

$$\mathrm{Fe}_\infty + \mathrm{Fe}_n \rightleftharpoons \mathrm{Fe}_{\infty+n}, \quad \mathrm{Fe}^{n+} \rightleftharpoons \mathrm{Fe}^{(n+1)+} + \mathrm{e}^-,$$

where Fe_∞ is the condensed matter. FIG. 4 shows the results for a specific magnetic field strength and density of condensed matter, adapted from [50]. One can refer to the original paper for more details and other cases.

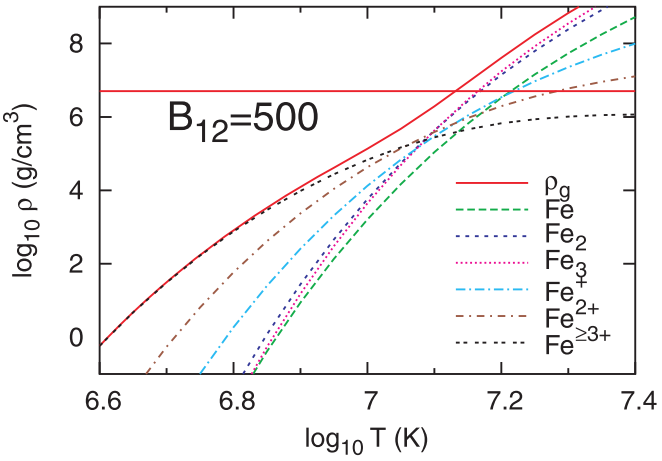

FIG. 4. The densities of the vapor (ρ_g) and its components in equilibrium with the condensed surface. The magnetic field is 500×10^{12} G. The horizontal line is the density ρ_s of the condensed matter, and the critical temperature is set by the condition $\rho_\mathrm{g} = \rho_\mathrm{s}$. Figure adapted from [50].

The nuclear matter inside the crust can also be affected by the magnetic field if the matter is in the strongly quantizing regime [1, p. 173], which means that most electrons are confined in the lowest Landau level. The condition is equivalent to the conjunction of temperature being much lower than $T_\mathrm{B} \coloneqq m_\mathrm{e}c^2 B_\star/k_\mathrm{B}$ (temperature corresponding to the cyclotron frequency) and the density being lower than a certain critical density ρ_B that only depends on the magnetic field, A, Z, and the number of free neutrons per nucleus. A comparison of the phase diagram with and without magnetic field is shown in FIG. 5, adapted from [1, p. 174].

By minimizing the energy per nucleon, one can also find that nuclei are less neutron-rich in higher magnetic fields [24]. The details of the calculation dot not involve much quantum many-body theory, so we will not discuss them in the present article, and one may refer to [24] for more details.

V. Superfluidity and superconductivity

In Bardeen–Cooper–Schrieffer (BCS) theory, if there is an attractive interaction between fermions, they may form Cooper pairs, which satisfy bosonic statistics [51]. In conventional superconductors, electrons are attracted through lattice phonon exchange and form Cooper pairs. The same mechanism does not work in the neutron star crust because the critical temperature would be too low to reach (estimated using the BCS weak coupling approximation) for such high density [38].

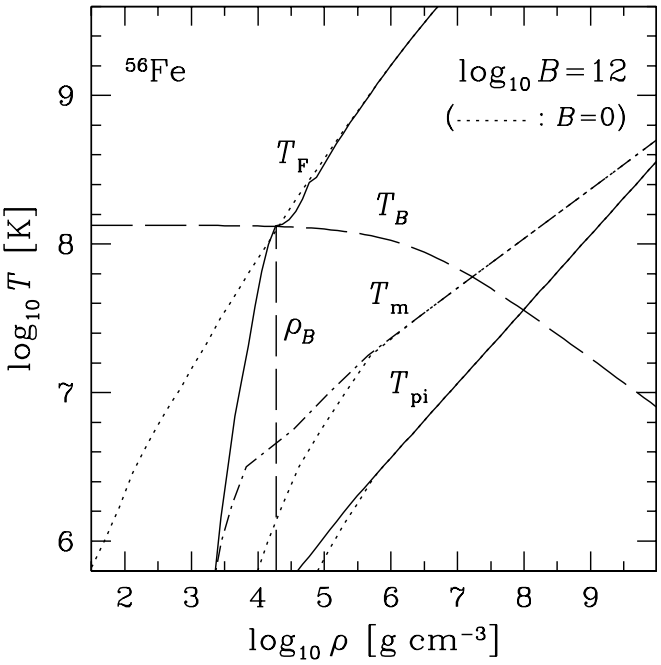

FIG. 5. Different parameter domains for ^{56}Fe plasma with magnetic field 10^{12} G. The dash-dot line is the melting line (corresponding to the classical plasma melting with $\Gamma_\mathrm{m} = 175$). The solid lines are electron Fermi temperature T_F and ion plasma temperature T_pi. The long-dash lines are $T_\mathrm{B}, \rho_\mathrm{B}$ marking different regimes (the definition of T_B is different from the main text beyond $\rho > \rho_\mathrm{B}$). The dotted lines are the case of zero magnetic field. Figure adapted from [38][a].

[a] In [38], it says the figure is from [1], but the version in [1, p. 174] is different. The better version here is from [38].

However, nucleons may form Cooper pairs in the crust, where the paring interaction is the strong interaction between nucleons, which is attractive in many JLS channels (J total angular momentum, L orbital angular momentum, S spin) [52]. Neutron Cooper pairs can form isotropic superfluid like ^{4}He, and proton Cooper pairs can form superconductor similar to conventional superconductors.

Because the interaction depends on angular momenta, the gap function is anisotropic (except for the simplest singlet S-wave). If we ignore the moment spin degrees of freedom and tensor interaction for simplicity, we can get the following equations for the partial-wave components of the gap function of neutrons [52]:

$$\Delta_L(k) = -\frac{1}{\pi}\int_0^\infty k'\,\mathrm{d}k'\,\frac{V_L(k,k')\,\Delta_L(k')}{\sqrt{\epsilon(k')^2 + \sum_{L'}\Delta_{L'}(k')^2}},$$

where $\epsilon(k)$ is the single-particle energy relative to the chemical potential; L labels the partial-wave component and represents orbital momentum; and $V_L(k,k')$ is the interaction. One can then derive the pairing gap by assuming a quadratic dispersion for the single-particle spectrum

$$\epsilon(k_i) = \frac{\hbar^2 k_i^2}{2m_{\mathrm{n}}^{\mathrm{eff}}} + \delta_i,$$

where i encodes quantum numbers, such as momentum, isospin projection, and spin. Note that these discussions are for the case of zero temperature, and the superfluidity disappears when the temperature is higher than the critical temperature T_{c}, which can be approximated by [53, p. 288]

$$\frac{\Delta(T=0)}{k_{\mathrm{B}}T_{\mathrm{c}}} = \pi \mathrm{e}^{-\gamma} \approx 1.76,$$

where γ is the Euler–Mascheroni constant.

A feature of superfluid is its quantized vortices: the momentum circulation over any closed path is quantized to [54]

$$\oint \mathbf{p} \cdot \mathrm{d}\mathbf{l} = 2\pi\hbar N, \quad N \in \mathbb{Z}.$$

These vortices are conjectured to be the origin of pulsar glitches [3]. Similarly, the superconductor formed by proton Cooper pairs quantizes the magnetic flux to form flux tubes [53, pp. 241–242]:

$$\oint \mathbf{A} \cdot \mathrm{d}\mathbf{l} = \frac{2\pi\hbar}{e} N, \quad N \in \mathbb{Z}.$$

The neutron vortices and the flux tubes can interact with each other and affect the dynamic evolution of the star [55].

VI. Conclusion

In this article, we have reviewed some of the quantum many-body theories that describe the crust of a neutron star.

The outer crust, with its lattice of nuclei surrounded by relativistic electrons, is governed by interactions modeled using one-component plasma theories. Meanwhile, the inner crust is defined by the neutron drip point, where free neutrons form Cooper pairs and exhibit superfluid behavior, with implications for pulsar glitches and other astrophysical phenomena.

Magnetic fields play a transformative role in neutron star crusts. They confine electrons to quantized Landau levels, altering the composition and phase transitions of crustal matter. Magnetic effects also induce unique condensed phases on the surface and influence the composition of nuclei in the inner crust, leading to deviations from standard neutron-rich configurations. These findings emphasize the critical interplay between quantum mechanics, strong interactions, and magnetism in extreme astrophysical environments.

[1] P. Haensel, A. Y. Potekhin, and D. G. Yakovlev, *Neutron stars 1: Equation of State and Structure* (Springer, 2007).

[2] V. M. Kaspi and A. M. Beloborodov, Magnetars, Annual Review of Astronomy and Astrophysics **55**, 261 (2017).

[3] B. Link, R. I. Epstein, and K. A. Van Riper, Pulsar glitches as probes of neutron star interiors, Nature **359**, 616 (1992).

[4] P. D. Lasky, Gravitational waves from neutron stars: A review, Publications of the Astronomical Society of Australia **32**, 10.1017/pasa.2015.35 (2015).

[5] D. A. Baiko and A. I. Chugunov, Breaking properties of neutron star crust, Monthly Notices of the Royal Astronomical Society **480**, 5511 (2018).

[6] E. J. Ferrer and A. Hackebill, Thermodynamics of neutrons in a magnetic field and its implications for neutron stars, Physical Review C **99**, 10.1103/physrevc.99.065803 (2019).

[7] A. I. Chugunov and D. G. Yakovlev, Shear viscosity and oscillations of neutron star crust, Astronomy Reports **49**, 724 (2005).

[8] N. Chamel and P. Haensel, Physics of neutron star crusts, Living Reviews in Relativity **11**, 10.12942/lrr-2008-10 (2008).

[9] C. J. Horowitz, J. Piekarewicz, and B. Reed, Insights into nuclear saturation density from parity-violating electron scattering, Physical Review C **102**, 10.1103/physrevc.102.044321 (2020).

[10] B. Hong, Nuclear matter under extreme conditions: From quark-gluon plasma to neutron stars, Journal of the Korean Physical Society **72**, 1515 (2018).

[11] W. C. Ho and C. O. Heinke, A neutron star with a carbon atmosphere in the cassiopeia a supernova remnant, Nature **462**, 71 (2009).

[12] V. S. Beskin, Radio pulsars, Physics-Uspekhi **42**, 1071 (1999).

[13] N. Chamel, A. F. Fantina, J. L. Zdunik, and P. Haensel, Neutron drip transition in accreting and nonaccreting neutron star crusts, Physical Review C **91**, 10.1103/physrevc.91.055803 (2015).

[14] G. Baym, C. Pethick, and P. Sutherland, The ground state of matter at high densities: equation of state and stellar models, Astrophysical Journal, vol. 170, p. 299 **170**, 299 (1971).

[15] A. Anders, S. Anders, A. Forster, and I. G. Brown, Pressure ionization: Its role in metal vapour vacuum arc plasmas and ion sources, Plasma Sources Science and Technology **1**, 263 (1992).

[16] J. P. Hansen, Statistical mechanics of dense ionized matter. i. equilibrium properties of the classical one-component plasma, Physical Review A **8**, 3096 (1973).

[17] D. H. Dubin, First-order anharmonic correction to the free energy of a coulomb crystal in periodic boundary conditions, Physical Review A **42**, 4972 (1990).

[18] G. Chabrier, N. W. Ashcroft, and H. E. DeWitt, White dwarfs as quantum crystals, Nature **360**, 48 (1992).

[19] G. Chabrier, Quantum effects in dense coulumbic matter: application to the cooling of white dwarfs, The Astrophysical Journal **414**, 695 (1993).

[20] M. D. Jones and D. M. Ceperley, Crystallization of the one-component plasma at finite temperature, Physical Review Letters **76**, 4572 (1996).

[21] J. M. Lattimer, Introduction to neutron stars, AIP Conference Proceedings **1645**, 61 (2015).

[22] R. A. Coldwell-Horsfall and A. A. Maradudin, Zero-point energy of an electron lattice, Journal of Mathematical Physics **1**, 395 (1960).

[23] D. Lunney, J. M. Pearson, and C. Thibault, Recent trends in the determination of nuclear masses, Reviews of Modern Physics **75**, 1021 (2003).

[24] J. M. Pearson, S. Goriely, and N. Chamel, Properties of the outer crust of neutron stars from hartree–fock–bogoliubov mass models, Physical Review C **83**, 10.1103/physrevc.83.065810 (2011).

[25] A. Burrows and J. M. Lattimer, On the accuracy of the single-nucleus approximation in the equation of state of hot, dense matter, Astrophysical Journal, Part 1 (ISSN 0004-637X), vol. 285, Oct. 1, 1984, p. 294-303. **285**, 294 (1984).

[26] C. J. Jog and R. A. Smith, Mixed lattice phases in cold dense matter, The Astrophysical Journal **253**, 839 (1982).

[27] M. Thoennessen, Reaching the limits of nuclear stability, Reports on Progress in Physics **67**, 1187 (2004).

[28] A. Bethe Hans and J. Pethick Christopher, Neutron star matter, Nucl. Phys. A **175**, 225 (1971).

[29] W. Kohn and L. J. Sham, Self-consistent equations including exchange and correlation effects, Physical Review **140**, 10.1103/physrev.140.a1133 (1965).

[30] S. Lundqvist and N. H. March, *Theory of the Inhomogeneous Electron Gas* (Plenum Press, 1983).

[31] M. Brack, C. Guet, and H.-B. Håkansson, Selfconsistent semiclassical description of average nuclear properties—a link between microscopic and macroscopic models, Physics Reports **123**, 275 (1985).

[32] I. Zahed and G. Brown, The skyrme model, Physics Reports **142**, 1 (1986).

[33] M. Onsi, A. K. Dutta, H. Chatri, S. Goriely, N. Chamel, and J. M. Pearson, Semi-classical equation of state and specific-heat expressions with proton shell corrections for the inner crust of a neutron star, Physical Review C **77**, 10.1103/physrevc.77.065805 (2008).

[34] J. W. Negele and D. Vautherin, Density-matrix expansion for an effective nuclear hamiltonian, Physical Review C **5**, 1472 (1972).

[35] J. W. Negele and D. Vautherin, Density-matrix expansion for an effective nuclear hamiltonian. ii, Physical Review C **11**, 1031 (1975).

[36] E. Wigner and F. Seitz, On the constitution of metallic sodium, Physical Review **43**, 804 (1933).

[37] M. Baldo, E. Saperstein, and S. Tolokonnikov, The role of the boundary conditions in the wigner–seitz approximation applied to the neutron star inner crust, Nuclear Physics A **775**, 235 (2006).

[38] N. Chamel and P. Haensel, Physics of neutron star crusts, Living Reviews in Relativity **11**, 10.12942/lrr-2008-10 (2008).

[39] J.-R. Buchler and Z. Barkat, Properties of low-density neutron-star matter, Physical Review Letters **27**, 48 (1971).

[40] R. Ogasawara and K. Sato, Nuclei in neutrino-degenerate dense matter. i: —cold case—, Progress of theoretical physics **68**, 222 (1982).

[41] K. Oyamatsu, Nuclear shapes in the inner crust of a neutron star, Nuclear Physics A **561**, 431 (1993).

[42] K. Sumiyoshi, K. Oyamatsu, and H. Toki, Neutron star profiles in the relativistic brueckner-hartree-fock theory, Nuclear Physics A **595**, 327 (1995).

[43] S. Goriely, M. Samyn, J. Pearson, and M. Onsi, Further explorations of skyrme–hartree–fock–bogoliubov mass formulas. iv: Neutron-matter constraint, Nuclear Physics A **750**, 425 (2005).

[44] J. W. Negele and D. Vautherin, Neutron star matter at sub-nuclear densities, Nuclear Physics A **207**, 298 (1973).

[45] M. Baldo, E. Saperstein, and S. Tolokonnikov, A realistic model of superfluidity in the neutron star inner crust, The European Physical Journal A **32**, 97 (2007).

[46] M. Baldo, E. Saperstein, and S. Tolokonnikov, Upper edge of the neutron star inner crust: The drip point and its vicinity, Physical Review C—Nuclear Physics **76**, 025803 (2007).

[47] M. Onsi, A. Dutta, H. Chatri, S. Goriely, N. Chamel, and J. Pearson, Semi-classical equation of state and specific-heat expressions with proton shell corrections for the inner crust of a neutron star, Physical Review C—Nuclear Physics **77**, 065805 (2008).

[48] M. Ruderman, Pulsars: structure and dynamics, Annual Review of Astronomy and Astrophysics, vol. 10, p. 427 **10**, 427 (1972).

[49] I. v. Rabi, Das freie elektron im homogenen magnetfeld nach der diracschen theorie, Zeitschrift für Physik **49**, 507 (1928).

[50] Z. Medin and D. Lai, Condensed surfaces of magnetic neutron stars, thermal surface emission, and particle acceleration above pulsar polar caps, Monthly Notices of the Royal Astronomical Society **382**, 1833 (2007).

[51] L. N. Cooper, Bound electron pairs in a degenerate fermi gas, Physical Review **104**, 1189 (1956).

[52] D. J. Dean and M. Hjorth-Jensen, Pairing in nuclear systems: From neutron stars to finite nuclei, Reviews of Modern Physics **75**, 607 (2003).

[53] J. R. Schrieffer, *Theory of superconductivity* (CRC Press, Taylor & Francis Group, 2018).

[54] L. Onsager, Statistical hydrodynamics, Il Nuovo Cimento (1943-1954) **6**, 279 (1949).

[55] M. Ruderman, T. Zhu, and K. Chen, Neutron star magnetic field evolution, crust movement, and glitches, The Astrophysical Journal **492**, 267 (1998).